

Matrix Infrared Spectrum and Aromaticity of the $\text{Al}_2(\text{CO})_2$ Molecule

Qinyu Kong, Mohua Chen, Jian Dong, Zhenhua Li, Kangnian Fan, and Mingfei Zhou*

Department of Chemistry and Laser Chemistry Institute, Fudan University, Shanghai 200433, People's Republic of China

Received: June 20, 2002; In Final Form: September 22, 2002

The reaction products between aluminum atoms and CO molecules in solid neon have been studied by matrix isolation infrared spectroscopy and quantum chemical calculations. Besides the previously reported AlCO and $\text{Al}(\text{CO})_2$ molecules, new absorption at 1727.9 cm^{-1} was also produced and assigned to a dibridged $\text{Al}_2(\text{CO})_2$ molecule based on isotopic substitution experiments and theoretical frequency calculations. High level ab initio computations indicated that the $\text{Al}_2(\text{CO})_2$ molecule has a singlet ground state with D_{2h} symmetry. The molecule exhibits characteristics of aromaticity with two completely delocalized π electrons and an appreciable diatropic ring current.

Introduction

Main group element carbonyls have attracted much interest as possible models for the chemical interaction of CO with main group element atoms in chemisorption studies and characterization of surface-adsorbed CO.^{1,2} The group 13 element carbonyls are among the most studied main group carbonyls both experimentally^{3–13} and theoretically.^{14–18} The neutral mono- and dicarbonyls of boron,^{3,4} aluminum,^{5–9} gallium, and indium^{9–12} have been prepared by reactions of element atoms with CO in solid matrixes and characterized by infrared absorption and electron paramagnetic resonance spectroscopy. The aluminum carbonyl anions have been prepared by codeposition of laser-ablated aluminum atoms and electrons with CO in excess argon.¹³ The group 13 element carbonyls have also been the subjects of a number of computational studies, which have provided very useful information on the spectra, structures, and bonding of these carbonyl species.^{14–18}

Under appropriate conditions, dinuclear carbonyl species such as $(\text{BCO})_2$,¹⁹ Al_2CO , $\text{Al}_2(\text{CO})_4$,⁸ Ga_2CO , In_2CO , $\text{Ga}_2(\text{CO})_2$, and $\text{In}_2(\text{CO})_2$ ¹² were also formed and characterized. It is very interesting to note that these dinuclear carbonyl species exhibited distinct structural and bonding character. The $(\text{BCO})_2$ molecule is linear with boron–boron multiply bonded.¹⁹ On the contrary, the $\text{Ga}_2(\text{CO})_2$ molecule is characterized as a planar dibridged carbonyl species and $\text{In}_2(\text{CO})_2$ is a loosely bound adduct best formulated as $\text{In}(\text{CO})_2 \cdot \text{In}$.¹² However, there is no previous evidence of $\text{Al}_2(\text{CO})_2$. In this paper, we report a combined matrix isolation Fourier transform infrared (FTIR) spectroscopic and theoretical study on the $\text{Al}_2(\text{CO})_2$ molecule.

Experimental and Computational Method

The experimental setup for pulsed laser ablation and matrix infrared spectroscopic investigation has been described previously.^{20,21} The 1064 nm fundamental of a Nd:YAG laser (20 Hz repetition rate and 8 ns pulse width) was focused onto the rotating Al target through a hole in a CsI window. The laser-ablated atoms were codeposited with CO in excess neon onto the 4 K CsI window for 30 min at a rate of 4–5 mmol/h.

* To whom correspondence should be addressed. E-mail: mfzhou@fudan.edu.cn.

TABLE 1: Product Absorptions (cm^{-1}) Observed for Laser-Abated Al Atom Codeposited with CO/Ne

assignment	^{12}CO	^{13}CO	$^{12}\text{CO} + ^{13}\text{CO}$
$\text{Al}(\text{CO})_2$	2001.9	1957.6	2001.9, 1984.6, 1957.6
$\text{Al}(\text{CO})_2$	1916.6	1873.5	1916.6, 1889.4, 1873.5
AlCO (site)	1889.4	1848.2	1889.4, 1848.2
AlCO	1882.9	1841.2	1882.9, 1841.2
$\text{Al}_2(\text{CO})_2$	1727.9	1691.5	1727.9, 1708.1, 1691.5

Typically, 5–10 mJ/pulse laser power was used. Carbon monoxide, $^{13}\text{C}^{16}\text{O}$ (Cambridge Isotope Laboratories), and a $^{12}\text{C}^{16}\text{O} + ^{13}\text{C}^{16}\text{O}$ mixture were used in different experiments. Infrared spectra were recorded on a Bruker Equinox 55 spectrometer at 0.5 cm^{-1} resolution using a DTGS detector. High-pressure mercury arc photolysis and matrix annealing were performed to aid assignments of the observed IR bands.

Quantum chemical calculations were performed to predict the structures and vibrational frequencies of the reaction products using the GAUSSIAN 98 program.²² Primary calculations were performed using the Becke's three parameter hybrid functional with the Lee–Yang–Parr correlation corrections (B3LYP).^{23,24} The 6-311+G(d) basis sets were used for C, O, and Al atoms.^{25,26} Geometries were fully optimized, and the vibrational frequencies were calculated with analytic second derivatives. For selected systems, coupled cluster calculations including triple excitations (CCSD(T)) were done with the 6-31+G(d) basis sets, and single point G3, G3S, G3SCB, and CCSD(T)/6-31+G(2df) calculations were carried out at the CCSD(T)/6-31+G(d) equilibrium geometries as well.^{27–29}

Results and Discussion

Infrared spectra in the C–O stretching vibrational frequency region from codeposition of laser-ablated Al and CO in excess neon are presented in Figure 1, and the product absorptions are listed in Table 1. Isotopic-substituted ^{13}CO and $^{12}\text{CO} + ^{13}\text{CO}$ samples were also used in different experiments, and typical spectra in the C–O stretching region are shown in Figure 2.

AlCO and $\text{Al}(\text{CO})_2$. The 1882.9 cm^{-1} band increased on annealing but decreased upon full mercury arc photolysis. It shifted to 1841.2 cm^{-1} with ^{13}CO and gave an isotopic 12/13 ratio of 1.0226. In the mixed $^{12}\text{CO} + ^{13}\text{CO}$ experiment, only

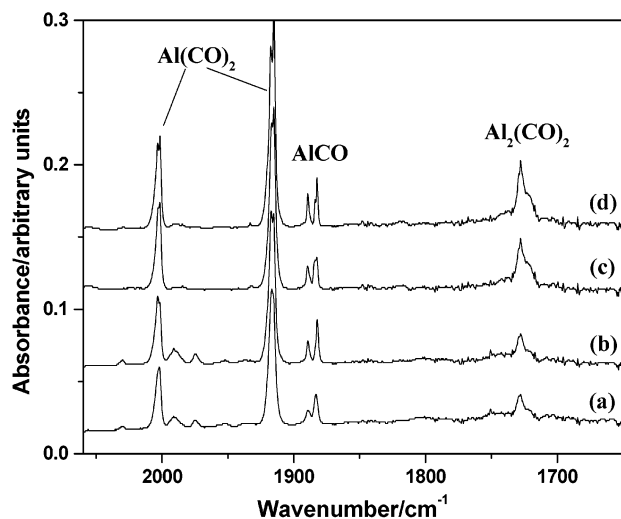


Figure 1. Infrared spectra in the 2060–1650 cm^{-1} region from codeposition of laser-ablated Al atoms with 0.2% CO in neon. (a) After sample deposition at 4 K, (b) after 8 K annealing, (c) after 10 min full Hg arc photolysis, and (d) after 10 K annealing.

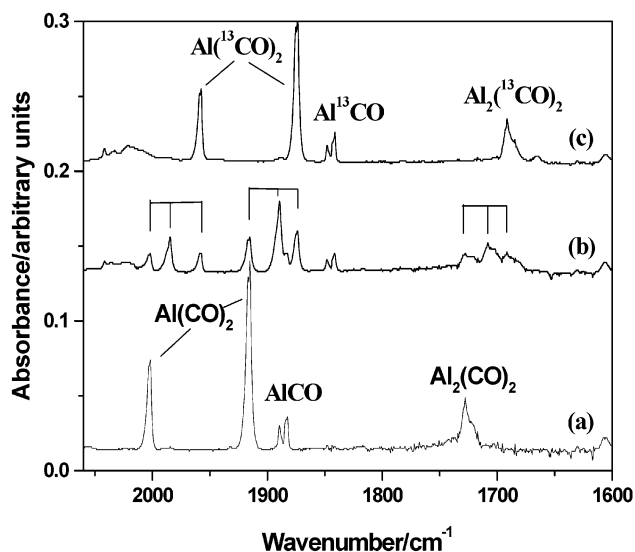


Figure 2. Infrared spectra in the 2060–1600 cm^{-1} region from codeposition of laser-ablated Al atoms with different matrix samples. (a) $^{12}\text{CO}/\text{Ne}$, (b) $^{12}\text{CO}/^{13}\text{CO}/\text{Ne}$, and (c) $^{13}\text{CO}/\text{Ne}$.

pure isotopic counterparts were presented, indicating that only one CO is involved in this vibrational mode. This band is assigned to the C–O stretching vibration of the AlCO molecule, which is in good agreement with previous argon matrix values.⁸ The band position in solid neon blue-shifted 15.2 cm^{-1} from the argon matrix value. The 2001.9 and 1916.6 cm^{-1} bands are assigned to the symmetric and antisymmetric C–O stretching vibrations of the $\text{Al}(\text{CO})_2$ molecule in solid neon. These two bands showed the same growth/decay characteristics on annealing or photolysis. In the mixed $^{12}\text{CO} + ^{13}\text{CO}$ experiment, both bands split into triplets at 2001.9/1984.6/1957.6 cm^{-1} and 1916.6/1889.4/1873.5 cm^{-1} with approximately 1:2:1 relative intensities, indicating the participation of two equivalent CO subunits. The vibrational frequencies in neon blue-shifted 6.8 and 9.2 cm^{-1} as compared to the argon matrix values.⁸

$\text{Al}_2(\text{CO})_2$. The band at 1727.9 cm^{-1} was weak upon deposition but increased markedly on full mercury arc photolysis. This band shifted to 1691.5 cm^{-1} with ^{13}CO . The isotopic 12/13 ratio of 1.0215 indicated that it is due to a C–O stretching vibration. In the mixed $^{12}\text{CO} + ^{13}\text{CO}$ experiment, this band split into a

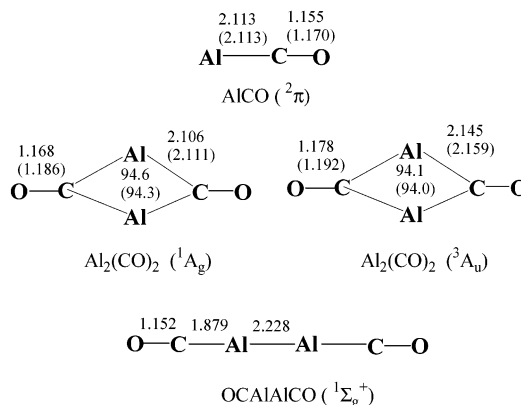


Figure 3. Optimized geometric parameters (bond length in Å, bond angle in degree) of AlCO, $\text{Al}_2(\text{CO})_2$, and OCAIAICO at the B3LYP/6-311+G(d) and CCSD(T)/6-31+G(d) (in parentheses) levels of theory.

triplet at 1727.9, 1708.1, and 1691.5 cm^{-1} with approximately 1:2:1 relative intensities (Figure 2). The triplet-mixed isotopic structure indicates the participation of two equivalent CO molecules in this mode. The vibrational frequency is too low for terminal carbonyls and is indicative of a bridged carbonyl. No absorption in the terminal C–O stretching frequency region associated with the 1727.9 cm^{-1} band was observed. Therefore, we assign the 1727.9 cm^{-1} band to the antisymmetric C–O stretching vibration of the dibridged $\text{Al}_2(\text{CO})_2$ molecule.

Quantum chemical computations support the experimental assignment and provide insight into the electronic structure and bonding in $\text{Al}_2(\text{CO})_2$. We performed theoretical calculations on both singlet and triplet potential energy surfaces for both terminal and bridged structures. The optimized structures are shown in Figure 3, and the vibrational frequencies and intensities are listed in Table 2. The primarily B3LYP/6-311+G(d) calculations indicate that the most stable structure is a dibridged triplet with D_{2h} symmetry, 6.1 kcal/mol lower in energy than the dibridged singlet. The linear OCAIAICO structure is predicted to be 49.4 kcal/mol higher in energy than the dibridged triplet and is a transition state with two imaginary vibrational frequencies corresponding to the bending mode. Both the singlet and the triplet dibridged structures exhibit Al–Al separations longer than the normal Al–Al single bond (the Al–Al bond length in ground state H_2AlAlH_2 was predicted to be 2.593 Å). This indicates that there is no direct bonding between two Al atoms. At the B3LYP/6-311+G(d) level of theory, the anti-symmetric C–O stretching vibration of dibridged triplet and singlet was predicted at 1717.7 and 1830.9 cm^{-1} , respectively, which are 11.5 cm^{-1} lower and 103.0 cm^{-1} higher than the experimental value of 1727.9 cm^{-1} in Ne. The calculated $^{12}\text{CO}/^{13}\text{CO}$ isotopic frequency ratios of 1.0213 (triplet) and 1.0219 (singlet) are about the same, and both fit the experimental value (1.0215). As listed in Table 2, frequency calculations offer little prospect of detecting any other infrared bands of $\text{Al}_2(\text{CO})_2$ in the experimental spectral range. We note that the B3LYP/6-311+G(d) method usually overestimates the vibrational frequencies of aluminum carbonyls. For example, the C–O stretching vibration of AlCO was observed at 1882.9 cm^{-1} in neon and was predicted at 1961.5 cm^{-1} . The symmetric and antisymmetric CO stretching vibrations of $\text{Al}(\text{CO})_2$ were predicted at 2059.5 and 1980.8 cm^{-1} but were observed at 2001.9 and 1916.6 cm^{-1} in solid neon. The bridged Al_2CO molecule has been reported in previous thermal atom reaction experiments, and the CO stretching mode was observed at 1737.1 cm^{-1} in solid argon.⁸ This molecule was predicted to have an $^3A'$ ground state with C_s symmetry.¹² The CO stretching

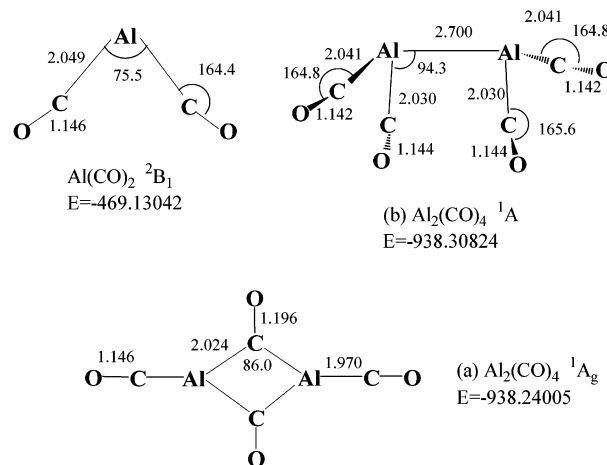
TABLE 2: Calculated Vibrational Frequencies (cm^{-1}) and Intensities (km/mol, in Parentheses) of the AlCO , $\text{Al}(\text{CO})_2$, Dibridged $\text{Al}_2(\text{CO})_2$, and OCAIAlCO Molecules at the B3LYP/6-311+G(d) Level (Vibrational Modes are Listed in Parentheses)

AlCO (${}^2\pi$)	$\text{Al}(\text{CO})_2$ (${}^2\text{B}_1$)	$\text{Al}_2(\text{CO})_2$ (${}^1\text{A}_g$)	$\text{Al}_2(\text{CO})_2$ (${}^3\text{A}_u$)	OCAIAlCO (${}^1\Sigma_g^+$)
1961.5 (862, σ)	2059.5 (647, a_1)	1908.2 (0, a_g)	1855.0 (0, a_g)	2042.0 (0, σ_g)
334.9 (18, σ)	1980.8 (1457, b_2)	1830.9 (1443, b_{1u})	1717.7 (1336, b_{1u})	2007.2 (4794, σ_u)
144.8 (10, π)	503.5 (39, a_1)	545.5 (0, b_{3g})	426.3 (9, b_{2u})	713.8 (0, σ_g)
	389.2 (1, b_2)	510.1 (0, b_{2g})	403.2 (0, b_{3g})	568.8 (70, σ_u)
	348.1 (1, a_1)	345.4 (0, a_g)	394.2 (0, b_{2g})	380.9 (1, π_u)
	315.6 (0, a_2)	331.3 (8, b_{1u})	328.9 (0, a_g)	309.7 (0, σ_g)
	296.2 (12, b_2)	279.8 (0, b_{3g})	304.8 (4, b_{1u})	239.2 (0, π_g)
	220.6 (1, b_1)	267.7 (8, b_{3u})	284.3 (0, b_{3g})	25.4 (4, π_u)
	85.9 (1, a_1)	246.9 (0, a_g)	280.5 (0, a_g)	255.0i (0, π_g)
		241.5 (10, b_{2u})	275.3 (2, b_{3u})	
		170.1 (3, b_{2u})	222.6 (3, b_{2u})	
		12.0 (5, b_{3u})	41.8 (1, b_{3u})	

mode was calculated at 1848.3 cm^{-1} . Therefore, we found that although the dibridged triplet is predicted to be lower in energy than the dibridged singlet, the calculated C–O stretching vibrational frequency of singlet fits the observed value better than that of the triplet.

To further ascertain the relative stability of the singlet and triplet, high level ab initio calculations were performed. We first did geometric optimization at the CCSD(T)/6-31+G(d) level, which indicated that the triplet was about 1.4 kcal/mol more stable than the singlet. We then carried out single point calculations with G3, G3S, G3SCB, and CCSD(T)/6-31+G-(2df) methods at the optimized geometries of the CCSD(T)/6-31+G(d) method. The singlet was calculated to be 1.6, 2.0, 2.8, and 0.2 kcal/mol lower in energy than the triplet, respectively. Therefore, we concluded that the ground state of $\text{Al}_2(\text{CO})_2$ is the ${}^1\text{A}_g$ singlet.

The low C–O stretching frequency of the $\text{Al}_2(\text{CO})_2$ molecule is parallel with the bridged dinuclear carbonyls of group 13 elements. In previous thermal Al atom experiments, absorption bands at 1737.1 and 470.5 cm^{-1} were assigned to the bridged Al_2CO molecule with C_{2v} symmetry.⁸ No similar band was observed in the present Al + CO/Ne experiments. Reactions of laser-ablated aluminum with CO in solid argon also failed to produce the Al_2CO molecule, probably due to low laser energy employed. In previous thermal Al atom reactions with CO in solid argon, another bimetallic species, $\text{Al}_2(\text{CO})_4$, was tentatively identified.⁸ This species was proposed to have planar structure with two terminal and two bridged CO subunits based upon the observation of two CO stretching absorptions: one in the bridging CO region at 1717.1 cm^{-1} involving two equivalent CO groups and another one in the terminal CO region around 1881.8 cm^{-1} . However, our experimental and theoretical results indicate that the $\text{Al}_2(\text{CO})_4$ assignment is probably in error. The 1717.1 cm^{-1} band increased on annealing in the present Al + CO/Ar experiments, but no absorption around 1881.8 cm^{-1} was observed. We suggest that the 1717.1 cm^{-1} band in solid argon matrix is the counterpart of the 1727.9 cm^{-1} band in solid neon and is due to the C–O stretching mode of the $\text{Al}_2(\text{CO})_2$ molecule. We performed density functional theory calculations on $\text{Al}_2(\text{CO})_4$. Two structures were considered as follows: one is a planar D_{2h} structure with two terminal and two bridged CO groups as previously suggested (Figure 4a), and the other is an Al–Al-bonded structure with four terminal CO subunits (Figure 4b). The planar D_{2h} structure is a transition state, while the Al–Al-bonded structure (C_2 symmetry) is a minimum. The energy of the D_{2h} structure is 42.2 kcal/mol higher than the C_2 structure. The C_2 structure lies 28.2 kcal/mol below the energy of two separated $\text{Al}(\text{CO})_2$, while the D_{2h} structure lies 14.0 kcal/mol above the energy of two separated $\text{Al}(\text{CO})_2$. As can be seen in Table 3, there are four C–O stretching vibrations of $\text{Al}_2(\text{CO})_4$

**Figure 4.** Optimized geometric parameters (bond length in Å, bond angle in degree) of $\text{Al}(\text{CO})_2$ and $\text{Al}_2(\text{CO})_4$ at the B3LYP/6-311+G(d) level of theory.**TABLE 3: Calculated Vibrational Frequencies (cm^{-1}) and Intensities (km/mol) of Two Forms of $\text{Al}_2(\text{CO})_4$ As Described in Figure 4**

	frequency (intensity, mode)
$\text{Al}_2(\text{CO})_4$ (${}^1\text{A}$)	2094.1 (523, a), 2053.9 (1973, b), 2044.7 (798, a), 2017.0 (452, b), 479.0 (17, a), 470.6 (16, b), 459.2 (6, b), 455.4 (1, a), 373.2 (8, a), 361.9 (10, b), 361.4 (1, a), 352.2 (12, b), 329.4 (20, b), 328.5 (9, a), 310.9 (3, a), 295.3 (8, b), 243.8 (1, a), 93.1 (0, a), 90.0 (0, b), 73.5 (3, b), 67.5 (1, a), 59.9 (0, a), 50.4 (1, b), 24.7 (0, a)
$\text{Al}_2(\text{CO})_4$ (${}^1\text{A}_g$)	2060.5 (0, a_g), 1999.3 (5713, b_{1u}), 1762.6 (0, a_g), 1717.0 (1402, b_{2u}), 566.7 (0, b_{3g}), 537.2 (41, b_{1u}), 531.9 (0, a_g), 519.8 (6, b_{2u}), 448.9 (0, b_{1g}), 396.2 (0, a_g), 364.7 (112, b_{1u}), 363.6 (0, b_{3g}), 354.1 (0, b_{3u}), 342.7 (0, b_{2g}), 341.9 (13, b_{2u}), 223.4 (0, a_g), 198.4 (14, b_{1u}), 169.8 (33, b_{3u}), 110.3 (0, b_{3g}), 71.3 (0, b_{2g}), 38.1 (0, b_{2u}), 29.8 (1, b_{3u}), 109.9i (0, b_{3g}), 140.6i (8, b_{3u})

with C_2 symmetry, and all are higher than 2000 cm^{-1} .

The $\text{Al}_2(\text{CO})_2$ molecule is aromatic based on structural, energetic, and magnetic criteria. The singlet $\text{Al}_2(\text{CO})_2$ ground state has an $\dots(8a_g)^2(4b_{2u})^2(2b_{3g})^2(2b_{3u})^2(1b_{2g})^2(6b_{1u})^2(5b_{2u})^2(9a_g)^2(3b_{3u})^2$ electronic configuration. The molecular orbital depictions in Figure 5 show that the highest occupied molecular orbital (HOMO) ($3b_{3u}$) of $\text{Al}_2(\text{CO})_2$ is a completely delocalized p_π orbital of the Al_2C_2 unit. Therefore, singlet $\text{Al}_2(\text{CO})_2$ possesses two π electrons, which satisfies the $4n + 2$ electron counting rule for aromatic compounds. From the structural point of view, $\text{Al}_2(\text{CO})_2$ has a rhombic D_{2h} symmetry with equal Al–C bond lengths. Consistent with its aromatic character,

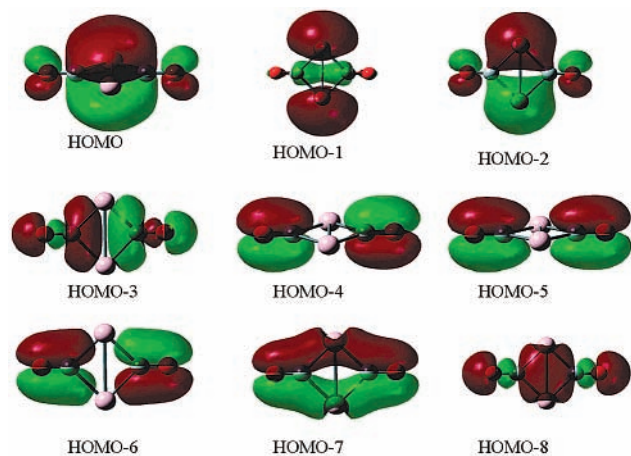


Figure 5. Valence molecular orbital depictions of dibridged singlet $\text{Al}_2(\text{CO})_2$.

TABLE 4: NICS (in ppm) at Ring Centers and 1 Å above Calculated at the GIAO/B3LYP/6-311+G(d) Level

molecule	NICS (x)	
	x = 0	x = 1
$\text{Al}_2(\text{CO})_2$ ($^1\text{A}_g$)	-16.70	-7.67
$\text{Al}_2(\text{CO})_2$ ($^3\text{A}_u$)	-4.47	-5.54
$\text{Ga}_2(\text{CO})_2$ ($^1\text{A}_g$)	-20.14	-10.41
$\text{Ga}_2(\text{CO})_2$ ($^3\text{A}_u$)	-5.20	-5.37
benzene	-8.02	-7.35

singlet $\text{Al}_2(\text{CO})_2$ is highly stabilized relative to the conceivable acyclic linear singlet OAlAlCO isomer. The magnetic properties of $\text{Al}_2(\text{CO})_2$ were assessed by computing the magnetic shieldings and converting them (by changing the sign) to nucleus-independent chemical shifts (NICS). The NICS index is now widely used to characterize aromaticity and antiaromaticity of various compounds with cyclically delocalized or localized electrons.^{30,31} Significantly negative NICS values in interior positions of rings reveal induced diatropic ring currents associated with “aromaticity” whereas positive values at each position denote paratropic ring currents and “antiaromaticity”. The calculated NICS at ring centers and 1 Å above are listed in Table 4. The NICS values show that singlet $\text{Al}_2(\text{CO})_2$ is aromatic, and the NICS(1) value, -7.67, is very close to the benzene value calculated at the same level. The triplet state $\text{Al}_2(\text{CO})_2$ has an $\dots(8a_g)^2(4b_{2u})^2(2b_{3g})^2(2b_{3u})^2(1b_{2g})^2(6b_{1u})^2(5b_{2u})^2(9a_g)^2(3b_{3u})^1(3b_{3g})^1$ electronic configuration. The singly occupied $3b_{3u}$ is a completely delocalized p_π orbital of the Al_2C_2 unit. Therefore, triplet $\text{Al}_2(\text{CO})_2$ possesses only one π electron. The SOMO ($3b_{3g}$) is a four center Al-C bonding orbital formed from the in-plane p orbitals. This σ molecular orbital also renders the $\text{Al}_2(\text{CO})_2$ molecule σ aromaticity. The triplet state is also aromatic but with smaller NICS values. Molecules with an odd number of π electrons are generally considered to be nonaromatic; however, an example of aromaticity with an odd number of π electrons has been reported very recently.³² The triplet $\text{Al}_2(\text{CO})_2$ molecule provides another example of aromaticity with an odd number of π electrons.

The dinuclear dicarbonyls of group 13 elements, B, Al, Ga, and In, exhibit stark bonding differences. The diboron dicarbonyl has been identified as a linear molecule with very short B-B bond distance (1.453 Å calculated at the (U)B3LYP/6-311+G(d) level).¹⁹ Although the dibridged structure is found to be a local minimum on the potential energy surface, it lies much higher in energy than the linear structure.¹⁹ As has been discussed, the relative stability between dibridged and linear structures was reversed in the Al case, and the linear structure

becomes a transition state. The digallium dicarbonyl exhibited the same bonding properties with the dialuminum dicarbonyl. The dibridged $\text{Ga}_2(\text{CO})_2$ molecule has been produced and identified in thermal gallium atom reactions with CO in solid argon.¹² We also did calculations on the dibridged $\text{Ga}_2(\text{CO})_2$ molecule, which shows the same valence electronic structure as the $\text{Al}_2(\text{CO})_2$ molecule. Both the singlet and the triplet state $\text{Ga}_2(\text{CO})_2$ molecules were predicted to be aromatic. As listed in Table 4, the calculated NICS values are about the same with that of $\text{Al}_2(\text{CO})_2$.

Recently, the cyclic Al_4^{2-} , Ga_4^{2-} , In_4^{2-} dianions and XAl_3^- (X = Si, Ge, Sn, and Pb) anions have been experimentally observed and characterized as aromatic species.^{33–35} Present investigations expand the aromaticity into neutral heterocyclic $\text{Al}_2(\text{CO})_2$ and $\text{Ga}_2(\text{CO})_2$ molecules, which may serve as building blocks of large clusters and related species.

Because no Al_2CO was observed in the present experimental conditions, the $\text{Al}_2(\text{CO})_2$ molecule was supposed to form via AlCO dimerization, which was computed to be exothermic by about 33.0 kcal/mol at the CCSD(T)/6-31+G(d) level. The increase of the $\text{Al}_2(\text{CO})_2$ absorption on photolysis at the expense of the AlCO absorption supports the proposed reaction mechanism.

Conclusions

The reactions between aluminum atoms and CO molecules have been reinvestigated in solid neon by FTIR spectroscopy and quantum chemical calculations. In agreement with previous argon matrix experiments, the primary reaction products are AlCO and $\text{Al}(\text{CO})_2$. New absorption at 1727.9 cm^{-1} is also produced and assigned to a dibridged $\text{Al}_2(\text{CO})_2$ molecule based on isotopic substitution experiments and theoretical frequency calculations. Density functional calculations imply that the $\text{Al}_2(\text{CO})_2$ molecule has a planar D_{2h} symmetry with the singlet and triplet states very close in energy. Although B3LYP/6-311+G(d) calculations predict the triplet state to be slightly lower in energy than the singlet, vibrational frequency analysis and high level ab initio calculations suggest a singlet ground state. Quantum chemical studies indicate that the singlet ground state of the $\text{Al}_2(\text{CO})_2$ molecule exhibits characteristics of aromaticity with two completely delocalized π electrons and an appreciable diatropic ring current.

Acknowledgment. We thank Professor Qizong Qin and Qike Zheng for help in experiments. This work is supported by NSFC (Grant 20003003 and 20125033) and the NKBRF of China.

References and Notes

- (1) Pirug, G.; Bonzel, H. P. *Surf. Sci.* **1988**, *199*, 371.
- (2) Li, P.; Xiang, Y.; Grassian, V. H.; Larsen, S. C. *J. Phys. Chem. B* **1999**, *103*, 5058.
- (3) Hamrick, Y. M.; Van Zee, R. J.; Godbout, J. T.; Weltner, W.; Lauderdale, W. J.; Stanton, J. F.; Bartlett, R. J. *J. Phys. Chem.* **1991**, *95*, 2840.
- (4) Burkholder, T. R.; Andrews, L. *J. Phys. Chem.* **1992**, *96*, 10195.
- (5) Hinchcliffe, A. J.; Ogden, J. S.; Oswald, D. D. *J. Chem. Soc., Chem. Commun.* **1972**, 338.
- (6) Kasai, P. H.; Jones, P. M. *J. Am. Chem. Soc.* **1984**, *106*, 8018. (b) Chenier, J. H. B.; Hampson, C. A.; Howard, J. A.; Mile, B.; Sutcliffe, R. *J. Phys. Chem.* **1986**, *90*, 1524.
- (7) Chenier, J. H. B.; Hampson, C. A.; Howard, J. A.; Mile, B. *J. Chem. Soc., Chem. Commun.* **1986**, 730.
- (8) Xu, C.; Manceron, L.; Perchard, J. P. *J. Chem. Soc., Faraday Trans.* **1993**, *89*, 1291.
- (9) Feltrin, A.; Guido, M.; Cesaro, S. N. *Vib. Spectrosc.* **1995**, *8*, 175.
- (10) Howard, J. A.; Sutcliffe, R.; Hampson, C. A.; Mile, B. *J. Phys. Chem.* **1986**, *90*, 4268.

- (11) Kasai, P. H.; Jones, P. M. *J. Phys. Chem.* **1985**, *89*, 2019. (b) Hatton, W. G.; Hacker, N. P.; Kasai, P. H. *J. Phys. Chem.* **1989**, *93*, 1328.
- (12) Himmel, H. J.; Downs, A. J.; Green, J. C.; Greene, T. M. *J. Phys. Chem. A* **2000**, *104*, 3642.
- (13) Zhang, L. N.; Dong, J.; Zhou, M. F.; Qin, Q. Z. *J. Chem. Phys.* **2000**, *113*, 10169.
- (14) Balaji, V.; Sunil, K. K.; Jordan, K. D. *Chem. Phys. Lett.* **1987**, *136*, 309.
- (15) (a) Bridgeman, A. J. *J. Chem. Soc., Dalton Trans.* **1997**, 1323. (b) Bridgeman, A. J. *Inorg. Chim. Acta.* **2001**, *321*, 27.
- (16) Skancke, A.; Liebman, J. F. *J. Phys. Chem.* **1994**, *98*, 13215.
- (17) (a) Wesolowski, S. S.; Crawford, T. D.; Fermann, J. T.; Schaefer, H. F. *J. Chem. Phys.* **1996**, *104*, 3672. (b) Wesolowski, S. S.; Galbraith, J. M.; Schaefer, H. F. *J. Chem. Phys.* **1998**, *108*, 9398.
- (18) Jursic, B. S. *Chem. Phys.* **1997**, *219*, 57.
- (19) Zhou, M. F.; Tsumori, N.; Li, Z. H.; Fan, K. N.; Andrews, L.; Xu, Q. *J. Am. Chem. Soc.* **2002**, *124*, 12936.
- (20) Chen, M. H.; Wang, X. F.; Zhang, L. N.; Yu, M.; Qin, Q. Z. *Chem. Phys.* **1999**, *242*, 81.
- (21) (a) Zhou, M. F.; Zhang, L. N.; Chen, M. H.; Qin, Q. Z. *J. Chem. Phys.* **2000**, *112*, 7089. (b) Zhou, M. F.; Zhang, L. N.; Qin, Q. Z. *J. Am. Chem. Soc.* **2000**, *122*, 4483.
- (22) Frisch, M. J.; Trucks, G. W.; Schlegel, H. B.; Scuseria, G. E.; Robb, M. A.; Cheeseman, J. R.; Zakrzewski, V. G.; Montgomery, J. A., Jr.; Stratmann, R. E.; Burant, J. C.; Dapprich, S.; Millam, J. M.; Daniels, A. D.; Kudin, K. N.; Strain, M. C.; Farkas, O.; Tomasi, J.; Barone, V.; Cossi, M.; Cammi, R.; Mennucci, B.; Pomelli, C.; Adamo, C.; Clifford, S.; Ochterski, J.; Petersson, G. A.; Ayala, P. Y.; Cui, Q.; Morokuma, K.; Malick, D. K.; Rabuck, A. D.; Raghavachari, K.; Foresman, J. B.; Cioslowski, J.; Ortiz, J. V.; Baboul, A. G.; Stefanov, B. B.; Liu, G.; Liashenko, A.; Piskorz, P.; Komaromi, I.; Gomperts, R.; Martin, R. L.; Fox, D. J.; Keith, T.; Al-Laham, M. A.; Peng, C. Y.; Nanayakkara, A.; Gonzalez, C.; Challacombe, M.; Gill, P. M. W.; Johnson, B.; Chen, W.; Wong, M. W.; Andres, J. L.; Gonzalez, C.; Head-Gordon, M.; Replogle, E. S.; Pople, J. A. *Gaussian 98*, revision A.7; Gaussian, Inc.: Pittsburgh, PA, 1998.
- (23) Becke, A. D. *J. Chem. Phys.* **1993**, *98*, 5648.
- (24) Lee, C.; Yang, E.; Parr, R. G. *Phys. Rev. B* **1988**, *37*, 785.
- (25) (a) McLean, A. D.; Chandler, G. S. *J. Chem. Phys.* **1980**, *72*, 5639. (b) Krishnan, R.; Binkley, J. S.; Seeger, R.; Pople, J. A. *J. Chem. Phys.* **1980**, *72*, 650.
- (26) (a) Wachter, J. H. *J. Chem. Phys.* **1970**, *52*, 1033. (b) Hay, P. J.; Wadt, W. R. *J. Chem. Phys.* **1985**, *82*, 299.
- (27) Curtiss, L. A.; Raghavachari, K.; Redfern, P. C.; Rassolov, V.; Pople, J. A. *J. Chem. Phys.* **1998**, *109*, 7764.
- (28) Curtiss, L. A.; Raghavachari, K.; Redfern, P. C.; Pople, J. A. *J. Chem. Phys.* **2000**, *112*, 1125.
- (29) Li, Z. H.; Wong, M. W. *Chem. Phys. Lett.* **2001**, *337*, 209.
- (30) Schleyer, P. v. R.; Maerker, C.; Dransfeld, A.; Jiao, H.; Hommes, N. J. R. v. E. *J. Am. Chem. Soc.* **1996**, *118*, 6317.
- (31) Schleyer, P. v. R.; Manoharan, M.; Wang, Z. X.; Kiran, B.; Jiao, H. J.; Puchta, R.; Hommes, N. J. R. v. E. *Org. Lett.* **2001**, *3*, 2465.
- (32) Zhou, M. F.; Xu, Q.; Wang, Z. X.; Schleyer, P. v. R. To be published.
- (33) Li, X.; Kuznetsov, A. E.; Zhang, H. F.; Boldyrev, A. I.; Wang, L. S. *Science* **2001**, *291*, 859.
- (34) Li, X.; Zhang, H. F.; Wang, L. S.; Kuznetsov, A. E.; Cannon, N. A.; Boldyrev, A. I. *Angew. Chem., Int. Ed.* **2001**, *40*, 1867.
- (35) Kuznetsov, A. E.; Boldyrev, A. I.; Li, X.; Wang, L. S. *J. Am. Chem. Soc.* **2001**, *123*, 8825.